



This is a repository copy of *Multi-carrier waveform design for directional modulation under peak to average power ratio constraint*.

White Rose Research Online URL for this paper:
<http://eprints.whiterose.ac.uk/143736/>

Version: Accepted Version

Article:

Zhang, B., Liu, W. orcid.org/0000-0003-2968-2888 and Li, Q. (2019) Multi-carrier waveform design for directional modulation under peak to average power ratio constraint. IEEE Access. ISSN 2169-3536

<https://doi.org/10.1109/access.2019.2904604>

© 2019 IEEE. Personal use of this material is permitted. Permission from IEEE must be obtained for all other users, including reprinting/ republishing this material for advertising or promotional purposes, creating new collective works for resale or redistribution to servers or lists, or reuse of any copyrighted components of this work in other works. Reproduced in accordance with the publisher's self-archiving policy.

Reuse

Items deposited in White Rose Research Online are protected by copyright, with all rights reserved unless indicated otherwise. They may be downloaded and/or printed for private study, or other acts as permitted by national copyright laws. The publisher or other rights holders may allow further reproduction and re-use of the full text version. This is indicated by the licence information on the White Rose Research Online record for the item.

Takedown

If you consider content in White Rose Research Online to be in breach of UK law, please notify us by emailing eprints@whiterose.ac.uk including the URL of the record and the reason for the withdrawal request.



eprints@whiterose.ac.uk
<https://eprints.whiterose.ac.uk/>

Date of publication xxxx 00, 0000, date of current version xxxx 00, 0000.

Digital Object Identifier 10.1109/ACCESS.2017.DOI

Multi-Carrier Waveform Design for Directional Modulation under Peak to Average Power Ratio Constraint

BO ZHANG¹, (MEMBER, IEEE), WEI LIU², (SENIOR MEMBER, IEEE), AND QIANG LI.³

¹College of Electronic and Communication Engineering, Tianjin Normal University, Tianjin, 300387, China (e-mail: b.zhangintj@outlook.com)

²Communications Research Group, Department of Electronic and Electrical Engineering, University of Sheffield, Sheffield S1 4ET, United Kingdom (e-mail: w.liu@sheffield.ac.uk)

³College of Information Engineering, Shenzhen University, Shenzhen 518060, China (e-mail: liqiang@szu.edu.cn)

Corresponding author: Bo Zhang (e-mail: b.zhangintj@outlook.com).

ABSTRACT Multi-carrier based waveform design for directional modulation (DM) is studied, where simultaneous data transmission over multiple frequencies can be achieved, with given phase distribution at the mainlobe and as random as possible over sidelobe regions for each frequency. The design can be implemented efficiently by the inverse discrete Fourier transform (IDFT) structure. However, the problem of multi-carrier design is the high peak to average power ratio (PAPR) of the resultant signals, leading to non-linear distortion when signal peaks pass through saturation regions of a power amplifier. To solve the problem, the $\text{PAPR} \leq \rho$ ($\rho \geq 1$) constraint is considered in the design and a solution called wideband beam and phase pattern formation by Newton's method (WBPFN) is proposed. The resultant beam patterns, phase patterns and complementary cumulative distribution function (CCDF) of PAPR are presented to demonstrate the effectiveness of the proposed design.

INDEX TERMS Directional modulation, multi-carrier, peak to average power ratio, phased antenna array

I. INTRODUCTION

IN the past few years, directional modulation (DM) has received more and more interest in the antenna array signal processing community. It was first introduced in [1], [2] using reflector switches to keep known constellation mappings in a desired direction or directions, and scramble them for the other directions. Then, a four-element reconfigurable antenna array was introduced by switching elements for each symbol to change its amplitude and phase of the element radiation pattern [3]. A method in [4] named dual beam DM was proposed to achieve DM, followed by phased array designs in [5]–[13]. In [14], a design with far-field radiation pattern templates was developed, along with a time modulation technique in [15], and an artificial-noise-aided zero-forcing synthesis approach in [16].

Recently, to increase channel capacity, a multi-carrier based design for DM was presented in [17], where multiple signals are transmitted at different frequencies simultaneously. The structure can be implemented efficiently using the inverse discrete Fourier transform (IDFT), and it allows different modulation schemes at different frequencies [17]. However, like traditional IDFT based multi-carrier wireless

communication systems, a potential problem of the multi-carrier design in [17] is the high peak to average power ratio (PAPR) when multiple signals are added together. If signal peaks pass through the non-linear (clipping) region of a power amplifier [18]–[26], then antenna performance will be seriously degraded. To avoid this, a PAPR constraint to control the signal envelope needs to be considered in the design.

Many methods have been proposed in traditional multi-carrier based communication to limit the PAPR of the transmitted signals. A clipping and filtering method was introduced in [27], [28], which iteratively limits the maximum amplitude until its corresponding output is under or equal to a pre-defined PAPR. Selective mapping (SLM) in [29], [30] was used to generate a set of phase sequences, and then each phase sequence is multiplied by the same data sequence to produce their corresponding transmitted sequences, and the one with the lowest PAPR is then chosen for transmission. In [31], [32], the partial transmit sequences (PTS) technique was studied, followed by the tone reservation method in [33] and tone injection method in [34]. The wideband beam pattern formation via iterative techniques (WBFIT) method was

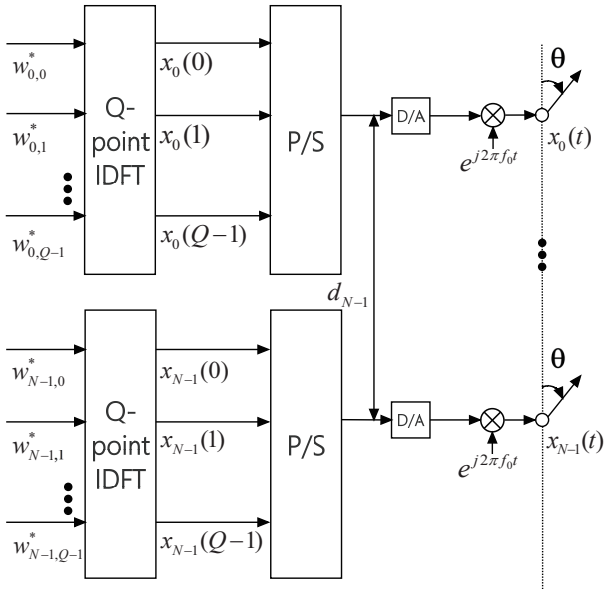


FIGURE 1: A multi-carrier based DM structure using an antenna array, where P/S denotes parallel to serial conversion.

introduced in [35] for wideband MIMO radar to directly link the beam pattern to the signals through their Fourier transform. However, the above mentioned methods do not consider different phase requirements for different regions of the pattern and for different symbols, and therefore can not be applied directly in our context. In this work, we propose a new method called wideband beam and phase pattern formation by Newton's method (WBPFN) to solve the PAPR and phase pattern formation problem simultaneously in the design of multi-carrier based DM antenna array system.

The remaining sections of this paper are organised as follows. A review of the multi-carrier based DM structure is given in Sec. II. The proposed method WBPFN to solve the $\text{PAPR} \leq \rho$ ($\rho \geq 1$) minimization problem for DM is described in Sec. III. In Sec. IV, design examples are presented, followed by conclusions in Sec. V.

II. REVIEW OF MULTI-CARRIER BASED DIRECTIONAL MODULATION

A linear antenna array for multi-carrier based DM implemented by the IDFT structure is shown in Fig. 1 [17], which consists of N omnidirectional antennas with spacing d_n between the zeroth and the n -th antenna for $n = 1, \dots, N-1$. Each antenna is associated with multiple frequency dependent weight coefficients $w_{n,q}$, $n = 0, \dots, N-1$ and $q = 0, \dots, Q-1$, where n and q represent the index of antenna and frequency, respectively. The transmission angle is represented by $\theta \in [0^\circ, 180^\circ]$.

As explained in [17], the steering vector of the array at the

q -th frequency is given by

$$\begin{aligned} \mathbf{s}(\omega_q, \theta) &= [1, e^{j\omega_q \tau_1}, \dots, e^{j\omega_q \tau_{N-1}}]^T \\ &= [1, e^{j2\pi(f_0 + (-\frac{Q}{2} + q)\Delta f)\tau_1}, \dots, \\ &\quad e^{j2\pi(f_0 + (-\frac{Q}{2} + q)\Delta f)\tau_{N-1}}]^T, \end{aligned} \quad (1)$$

where $\{\cdot\}^T$ represents transpose, $\tau_n = \frac{d_n \cos(\theta)}{c}$ is the time advance between the zeroth and n -th antennas. The beam response of the array at the q -th frequency is given by

$$p(\omega_q, \theta) = \mathbf{w}^H(\omega_q) \mathbf{s}(\omega_q, \theta), \quad (2)$$

where $\{\cdot\}^H$ represents the Hermitian transpose, and $\mathbf{w}(\omega_q)$ is the weight vector at the q -th frequency

$$\mathbf{w}(\omega_q) = [w_{0,q}, w_{1,q}, \dots, w_{N-1,q}]^T. \quad (3)$$

In the context of DM, for M -ary signaling, we define $p_m(\omega_q, \theta)$ as the desired array response for the m -th constellation point ($m = 0, \dots, M-1$) at the q -th frequency, with its corresponding weight vector $\mathbf{w}_m(\omega_q) = [w_{m,0,q}, \dots, w_{m,N-1,q}]^T$. We sample the whole angle range of interest by R points, with r points in the mainlobe and $R-r$ points $\theta_0, \theta_1, \dots, \theta_{R-r-1}$ in the sidelobe [17]. Then, we can construct the following two vectors

$$\begin{aligned} \mathbf{P}_m(\omega_q, \theta_{SL}) &= [p_m(\omega_q, \theta_0), p_m(\omega_q, \theta_1), \dots, \\ &\quad p_m(\omega_q, \theta_{R-r-1})], \\ \mathbf{P}_m(\omega_q, \theta_{ML}) &= [p_m(\omega_q, \theta_{R-r}), p_m(\omega_q, \theta_{R-r+1}), \dots, \\ &\quad p_m(\omega_q, \theta_{R-1})]. \end{aligned} \quad (4)$$

Accordingly, at the q -th frequency, all steering vectors at sidelobe regions form the $N \times (R-r)$ matrix $\mathbf{S}(\omega_q, \theta_{SL})$, and all vectors in desired directions form the $N \times r$ matrix $\mathbf{S}(\omega_q, \theta_{ML})$.

Then for the m -th constellation point at the q -th frequency, the weight coefficients can be obtained by

$$\begin{aligned} \min_{\mathbf{w}_m(\omega_q)} \quad & \|\mathbf{p}_m(\omega_q, \theta_{SL}) - \mathbf{w}_m^H(\omega_q) \mathbf{S}(\omega_q, \theta_{SL})\|_2 \\ \text{subject to} \quad & \mathbf{w}_m^H(\omega_q) \mathbf{S}(\omega_q, \theta_{ML}) = \mathbf{p}_m(\omega_q, \theta_{ML}). \end{aligned} \quad (5)$$

The problem in (5) can be solved by the method of Lagrange multipliers [17] and the optimum value for the weight vector $\mathbf{w}_m(\omega_q)$ is given in the following,

$$\begin{aligned} \mathbf{w}_m(\omega_q) &= \mathbf{R}^{-1}(\mathbf{S}(\omega_q, \theta_{SL}) \mathbf{P}_m^H(\omega_q, \theta_{SL}) - \mathbf{S}(\omega_q, \theta_{ML}) \\ &\quad \times ((\mathbf{S}^H(\omega_q, \theta_{ML}) \mathbf{R}^{-1} \mathbf{S}(\omega_q, \theta_{ML}))^{-1} \\ &\quad (\mathbf{S}^H(\omega_q, \theta_{ML}) \mathbf{R}^{-1} \mathbf{S}(\omega_q, \theta_{SL}) \mathbf{P}_m^H(\omega_q, \theta_{SL}) \\ &\quad - \mathbf{P}_m^H(\omega_q, \theta_{ML}))), \end{aligned} \quad (6)$$

where $\mathbf{R} = \mathbf{S}(\omega_q, \theta_{SL}) \mathbf{S}^H(\omega_q, \theta_{SL})$.

III. PAPR CONSTRAINT

Although the IDFT based DM shown in Fig. 1 works well in theory, in practice we need to consider the PAPR problem, where due to signal envelope fluctuation, signal peaks can fall into saturation regions of an amplifier, resulting in non-linear

distortion. The PAPR of the output signal at the n -th antenna can be defined as [19], [23]–[26]

$$\begin{aligned} \text{PAPR}(\mathbf{x}_n) &= \frac{\max_{k=0, \dots, Q-1} |x_n(k)|^2}{\frac{1}{Q} \sum_{k=0}^{Q-1} |x_n(k)|^2} \\ &= \frac{\|\mathbf{x}_n\|_\infty^2}{\frac{1}{Q} \|\mathbf{x}_n\|_2^2} \quad n = 0, 1, \dots, N-1, \end{aligned} \quad (7)$$

where $\mathbf{x}_n = [x_n(0), \dots, x_n(Q-1)]$. Here the design in (5) for a particular constellation point at a particular frequency can be extended to the following, where cost functions and constraints for all constellation points at all frequencies are considered together [17]

$$\begin{aligned} \min_{\mathbf{W}} \quad & \|\mathbf{P}_{SL} - \mathbf{W}^H \mathbf{S}_{SL}\|_2 \\ \text{subject to} \quad & \mathbf{W}^H \mathbf{S}_{ML} = \mathbf{P}_{ML}, \end{aligned} \quad (8)$$

where

$$\begin{aligned} \mathbf{W} &= \text{blkdiag}\{\mathbf{W}(\omega_0), \dots, \mathbf{W}(\omega_{Q-1})\}, \\ \mathbf{P}_{SL} &= \text{blkdiag}\{\mathbf{P}_{SL}(\omega_0, \theta_{SL}), \dots, \mathbf{P}_{SL}(\omega_{Q-1}, \theta_{SL})\}, \\ \mathbf{P}_{ML} &= \text{blkdiag}\{\mathbf{p}_{ML}(\omega_0, \theta_{ML}), \dots, \mathbf{p}_{ML}(\omega_{Q-1}, \theta_{ML})\}, \\ \mathbf{S}_{SL} &= \text{blkdiag}\{\mathbf{S}(\omega_0, \theta_{SL}), \dots, \mathbf{S}(\omega_{Q-1}, \theta_{SL})\}, \\ \mathbf{S}_{ML} &= \text{blkdiag}\{\mathbf{s}(\omega_0, \theta_{ML}), \dots, \mathbf{s}(\omega_{Q-1}, \theta_{ML})\}, \\ \mathbf{W}(\omega_q) &= [\mathbf{w}_0(\omega_q), \dots, \mathbf{w}_{M-1}(\omega_q)], \\ \mathbf{P}_{SL}(\omega_q, \theta_{SL}) &= [\mathbf{p}_0(\omega_q, \theta_{SL}), \dots, \mathbf{p}_{M-1}(\omega_q, \theta_{SL})]^T, \\ \mathbf{P}_{ML}(\omega_q, \theta_{ML}) &= [\mathbf{p}_0(\omega_q, \theta_{ML}), \dots, \mathbf{p}_{M-1}(\omega_q, \theta_{ML})]^T. \end{aligned} \quad (9)$$

As the PAPR constraint is designed for all antennas and each antenna has Q frequency dependent weight coefficients, the formulation for DM design subject to the PAPR constraint is given by

$$\begin{aligned} \min_{\mathbf{W}} \quad & \|\mathbf{P}_{SL} - \mathbf{W}^H \mathbf{S}_{SL}\|_2 \\ \text{subject to} \quad & \mathbf{W}^H \mathbf{S}_{ML} = \mathbf{P}_{ML} \\ & \|\mathbf{x}_n\|_2^2 = \hat{Q} \\ & \text{PAPR}(\mathbf{x}_n) \leq \rho \quad n = 0, \dots, N-1. \end{aligned} \quad (10)$$

where ρ ($\rho \geq 1$) represents the upper bound of PAPR. Here, an energy constraint $\|\mathbf{x}_n\|_2^2 = \hat{Q}$ is imposed [35] for the PAPR requirements (although \hat{Q} can be any values, $\hat{Q} = Q$ is chosen to make the denominator of (7) equal to one for simplicity). Then, based on the constraint $\|\mathbf{x}_n\|_2^2 = \hat{Q} = Q$, $\text{PAPR}(\mathbf{x}_n) \leq \rho$ can be changed to

$$\max_{k=0, \dots, Q-1} |x_n(k)|^2 \leq \rho. \quad (11)$$

However, (10) is nonconvex because of the PAPR constraint. For example, for $\rho = 1$, each of $[x_n(0), \dots, x_n(Q-1)]$ in \mathbf{x}_n can only take values from the unit circle [35], which does not satisfy a convex set. To solve the problem, the WBPFN method is proposed, which includes two stages. At the first stage, the coefficients in (8) without considering the PAPR constraint are first calculated, and are used to construct a 3-D matrix. At the second stage, a set of auxiliary

variables $\{\psi_q\}_{q=-Q/2}^{Q/2-1}$ is introduced and is multiplied by the 3-D matrix. Then, based on the result, the weight coefficients are optimized iteratively until the given phase and PAPR requirements in the desired directions are satisfied.

Note that the main difference between our proposed method in (10) and the WBFIT method [35] in (12) is the additional phase requirement to the desired directions in our design.

$$\begin{aligned} \min_{\mathbf{x}_n} \quad & \|\mathbf{u}_n - \mathbf{x}_n\|_2 \\ \text{subject to} \quad & \|\mathbf{x}_n\|_2^2 = \hat{Q} \\ & \text{PAPR}(\mathbf{x}_n) \leq \rho \quad n = 0, \dots, N-1, \end{aligned} \quad (12)$$

where \mathbf{u}_n is a reference vector. Therefore, the newly formulated design problem cannot be solved by the original WBFIT method in [35].

A. STAGE ONE

The PAPR constraint is designed for \mathbf{x}_n , $n = 0, 1, \dots, N-1$, corresponding to the n -th antenna, and as shown in Fig. 1, each antenna is associated with Q frequency dependent inputs (weight coefficients) $[w_{n,0}^*, w_{n,1}^*, \dots, w_{n,Q-1}^*]$, resulting in Q outputs $[x_n(0), \dots, x_n(Q-1)]$ by IDFT [17]. Then, in the context of M -ary signaling for each frequency, there are M^Q sets of inputs (weight coefficients) for all Q frequencies, and each set contains $N \times Q$ coefficients. Then an $N \times Q \times M^Q$ matrix $\hat{\mathbf{W}}$ can be constructed to represent all sets of inputs, with $\hat{\mathbf{W}}(n, :, u)$ representing the inputs of the IDFT structure at the n -th antenna for the u -th set of coefficients. Details of constructing the 3-D matrix are described as follows

- 1) Calculate the values of weight coefficients $\mathbf{w}_m(\omega_q)$ for $m = 0, \dots, M-1$ and $q = 0, \dots, Q-1$ in (8).
- 2) Select one set of weight coefficients (an $N \times 1$ vector) from each frequency (e.g. for the q -th sub-carrier frequency, select one column from $[\mathbf{w}_0(\omega_q), \dots, \mathbf{w}_{M-1}(\omega_q)]$), and combine them together to form an $N \times Q$ matrix for all Q frequencies, representing one set of inputs of the IDFT. Then, with all M^Q sets of inputs, the $N \times Q \times M^Q$ matrix $\hat{\mathbf{W}}$ is constructed.

B. STAGE TWO

The objective of the WBPFN method is to find appropriate weight coefficients for each set of inputs that satisfy DM with their corresponding IDFT outputs \mathbf{x}_n subject to the PAPR constraints simultaneously. To achieve this, a set of auxiliary variables $\{\psi_q\}_{q=-Q/2}^{Q/2-1}$ is introduced. Details of the second stage are given below.

- 1) For the u -th set of inputs $\hat{\mathbf{W}}(:, :, u)$, $u = 0, \dots, M^Q - 1$, $\{\psi_q\}_{q=-Q/2}^{Q/2-1}$ are randomly generated following a uniform distribution within $[0, 2\pi]$.
- 2) Form the matrix $\mathbf{E} = \text{diag}\{e^{j\psi_{-Q/2}}, \dots, e^{j\psi_{Q/2-1}}\}$ and minimize the difference between $\mathbf{E}\hat{\mathbf{W}}^H(:, :, u)$

and the DFT of \mathbf{X} , subject to $\text{PAPR} \leq \rho$ ($\rho \geq 1$), i.e.

$$\begin{aligned} \min_{\mathbf{X}} \quad & \|\mathbf{E}\hat{\mathbf{W}}^H(:, :, u) - \mathbf{F}\mathbf{X}\|_2 \\ \text{subject to} \quad & \text{angle}((\mathbf{F}\mathbf{X})(q, :, u)\mathbf{S}(\omega_q, \theta_{ML})) \\ & = \text{angle}(\hat{\mathbf{W}}^H(q, :, u)\mathbf{S}(\omega_q, \theta_{ML})) \\ & \|\mathbf{x}_n\|_2^2 = \hat{Q} \\ & \text{PAPR}(\mathbf{x}_n) \leq \rho \text{ for } n = 0, \dots, N-1, \end{aligned} \quad (13)$$

where

$$\mathbf{F} = [\text{dft}_{-Q/2}, \dots, \text{dft}_{Q/2-1}]^T, \quad (14)$$

$$\begin{aligned} \text{dft}_q = & [1, e^{-j2\pi q/Q}, \dots, e^{-j2\pi \frac{(Q-1)q}{Q}}] \\ \text{for } q = & -Q/2, \dots, Q/2-1, \end{aligned} \quad (15)$$

$$\mathbf{X} = [\mathbf{x}_0, \mathbf{x}_1, \dots, \mathbf{x}_{N-1}], \quad (16)$$

$$\mathbf{x}_n = [x_n(0), x_n(1), \dots, x_n(Q-1)]^T. \quad (17)$$

Here, the proposed phase constraint

$$\begin{aligned} \text{angle}((\mathbf{F}\mathbf{X})(q, :, u)\mathbf{S}(\omega_q, \theta_{ML})) \\ = \text{angle}(\hat{\mathbf{W}}^H(q, :, u)\mathbf{S}(\omega_q, \theta_{ML})) \end{aligned} \quad (18)$$

is introduced to represent a phase equalization in the desired directions between the designed phases $\text{angle}((\mathbf{F}\mathbf{X})(q, :, u)\mathbf{S}(\omega_q, \theta_{ML}))$ and the corresponding desired phases $\text{angle}(\hat{\mathbf{W}}^H(q, :, u)\mathbf{S}(\omega_q, \theta_{ML}))$.

- 3) Similar to [35], the cost function in (13) is further changed to find the minimization for the corresponding n -th antenna, $n = 0, \dots, N-1$,

$$\begin{aligned} \|\mathbf{E}\hat{\mathbf{W}}^H(n, :, u) - \mathbf{F}\mathbf{x}_n\|_2 \\ = \|\frac{1}{Q}\mathbf{F}^H\mathbf{E}\hat{\mathbf{W}}^H(n, :, u) - \mathbf{x}_n\|_2. \end{aligned} \quad (19)$$

Then (13) changes to

$$\begin{aligned} \min_{\mathbf{x}_n} \quad & \|\frac{1}{Q}\mathbf{F}^H\mathbf{E}\hat{\mathbf{W}}^H(n, :, u) - \mathbf{x}_n\|_2 \\ \text{subject to} \quad & \text{angle}((\mathbf{F}\mathbf{X})(q, :, u)\mathbf{S}(\omega_q, \theta_{ML})) \\ & = \text{angle}(\hat{\mathbf{W}}^H(q, :, u)\mathbf{S}(\omega_q, \theta_{ML})) \\ & \|\mathbf{x}_n\|_2^2 = \hat{Q} \\ & \text{PAPR}(\mathbf{x}_n) \leq \rho \text{ for } n = 0, \dots, N-1. \end{aligned} \quad (20)$$

- 4) The problem in (20) can be solved by the ‘nearest-vector’ method in [35]–[37] in combination with the Newton’s method for the phase requirement in desired directions.

According to the nearest-vector solution, we first obtain \mathbf{x}_n subject to the constraint $\|\mathbf{x}_n\|_2^2 = \hat{Q}$, which is

$$\mathbf{x}_n = \sqrt{\hat{Q}} \frac{\frac{1}{Q}\mathbf{F}^H\mathbf{E}\hat{\mathbf{W}}^H(n, :, u)}{\|\frac{1}{Q}\mathbf{F}^H\mathbf{E}\hat{\mathbf{W}}^H(n, :, u)\|_2}. \quad (21)$$

With the PAPR constraint ($\max|\mathbf{x}_n| \leq \sqrt{\rho}$), if the magnitudes of all elements in \mathbf{x}_n are less than or equal to $\sqrt{\rho}$, then \mathbf{x}_n is a solution; otherwise, the element in \mathbf{x}_n corresponding to the largest element in magnitude in $\frac{1}{Q}\mathbf{F}^H\mathbf{E}\hat{\mathbf{W}}^H(n, :, u)$, represented by s_a , is given by $\sqrt{\rho}e^{j\text{angle}(s_a)}$ and the rest of the $Q-1$ elements in \mathbf{x}_n is calculated by (20); in other words, we re-run step 4 for the rest of the $Q-1$ elements. Here the difference is that the size of \mathbf{x}_n and $\frac{1}{Q}\mathbf{F}^H\mathbf{E}\hat{\mathbf{W}}^H(n, :, u)$ in (20) becomes $(Q-1) \times 1$, instead of the original $Q \times 1$, and the energy constraint changes to $\|\mathbf{x}_n\|_2^2 = \hat{Q} - \rho$. If the PAPR constraint is still not satisfied by the new results, we set the value of the largest element in \mathbf{x}_n (size $(Q-1) \times 1$ in this iteration) in the same way as in the previous iteration, and re-run step 4 for the rest of the $Q-2$ elements, and so on. The iterative process ends when the PAPR constraint is satisfied [36], [37].

- 5) Now we consider the phase requirement at the desired directions.

Based on the new weight coefficients, which are the DFT of \mathbf{X} calculated in the previous step, if the phase constraint

$$\begin{aligned} \text{angle}((\mathbf{F}\mathbf{X})(q, :, u)\mathbf{S}(\omega_q, \theta_{ML})) \\ - \text{angle}(\hat{\mathbf{W}}^H(q, :, u)\mathbf{S}(\omega_q, \theta_{ML})) = 0 \end{aligned} \quad (22)$$

is satisfied, then the desired phase pattern in the main-lobe direction based on the new coefficients subject to the PAPR constraint is achieved, and $\{\psi_q\}_{q=-Q/2}^{Q/2-1}$ is the proper set of auxiliary values, and we set $u = u+1$ and go back to step 1 for the $(u+1)$ -th set of inputs. If not, then we set

$$\{\psi_q\}_{q=-Q/2}^{Q/2-1} = \{\psi_q\}_{q=-Q/2}^{Q/2-1} - \frac{f(\{\psi_q\}_{q=-Q/2}^{Q/2-1})}{f'(\{\psi_q\}_{q=-Q/2}^{Q/2-1})}, \quad (23)$$

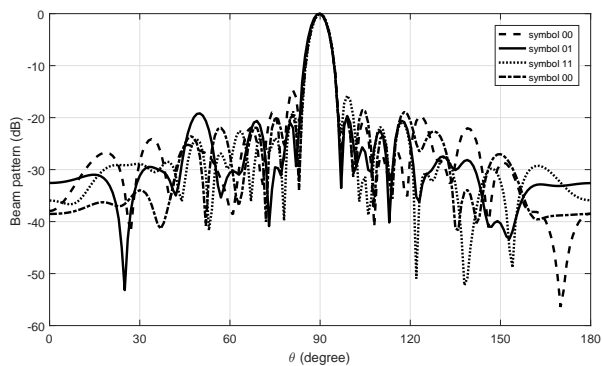
where

$$\begin{aligned} f(\{\psi_q\}_{q=-Q/2}^{Q/2-1}) = \text{angle}((\mathbf{F}\mathbf{X})(q, :, u)\mathbf{S}(\omega_q, \theta_{ML})) \\ - \text{angle}(\hat{\mathbf{W}}^H(q, :, u)\mathbf{S}(\omega_q, \theta_{ML})), \end{aligned} \quad (24)$$

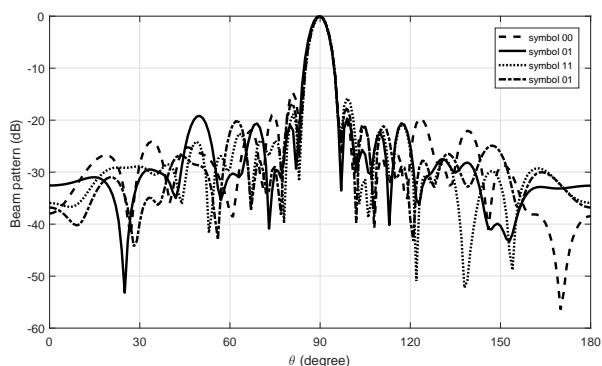
and run from steps 2 to 5 iteratively until the phase constraint in step 5 has been met. Here we have used the Newton’s method to optimize $\{\psi_q\}_{q=-Q/2}^{Q/2-1}$ to limit the corresponding phase differences (the left side of (22)) to be smaller than itself in the previous iteration. Note: $\{\psi_q\}_{q=-Q/2}^{Q/2-1}$ on the right side of (23) represents the previous value and on the left side denotes the latest value. The value of the denominator $f'(\{\psi_q\}_{q=-Q/2}^{Q/2-1})$ is selected by trial and error.

IV. DESIGN EXAMPLES

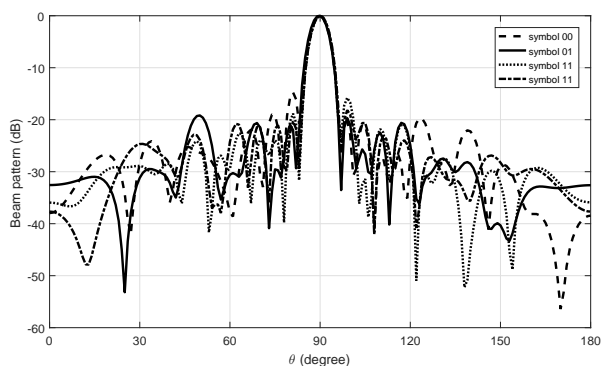
In this section, examples are provided based on a 20-element uniform linear antenna array (ULA) with and without $\text{PAPR} \leq \rho$ ($\rho \geq 1$) constraints to show the effectiveness of the proposed solution. Both broadside and off-broadside



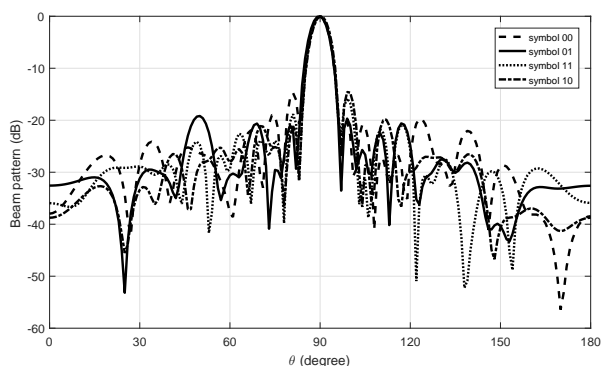
(a)



(b)



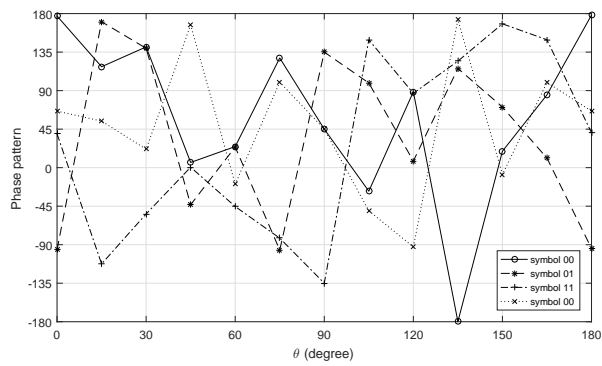
(c)



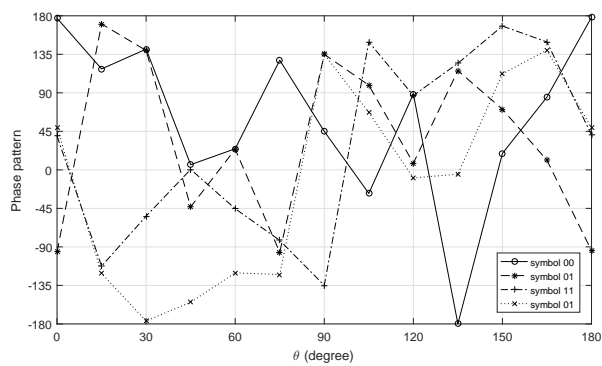
(d)

FIGURE 2: Resultant beam responses based on the broad-side design using eq. (5) for symbols (a) ‘00,01,11,00’, (b) ‘00,01,11,01’, (c) ‘00,01,11,11’, (d) ‘00,01,11,10’ without PAPR constraint.

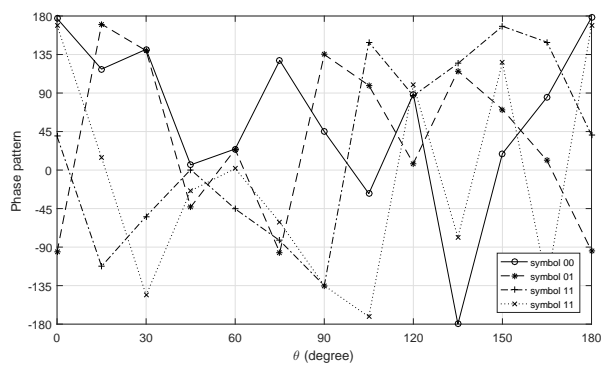
VOLUME 4, 2016



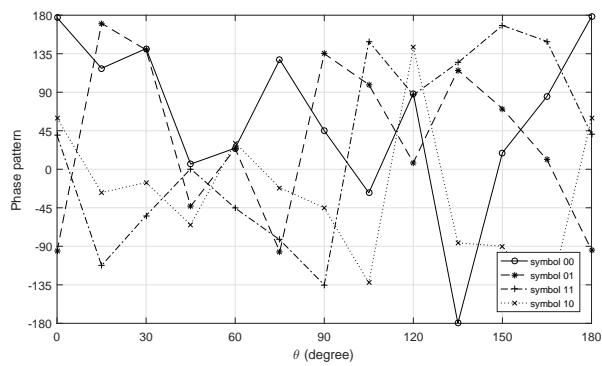
(a)



(b)



(c)



(d)

FIGURE 3: Resultant phase patterns based on the broad-side design using eq. (5) for symbols (a) ‘00,01,11,00’, (b) ‘00,01,11,01’, (c) ‘00,01,11,11’, (d) ‘00,01,11,10’ without PAPR constraint.

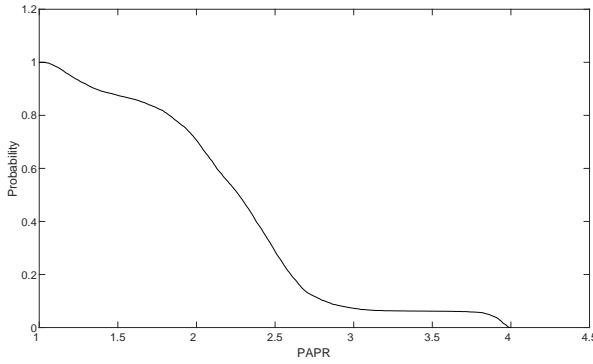


FIGURE 4: CCDF of PAPR based on the broadside design using eq. (5) without PAPR constraint.

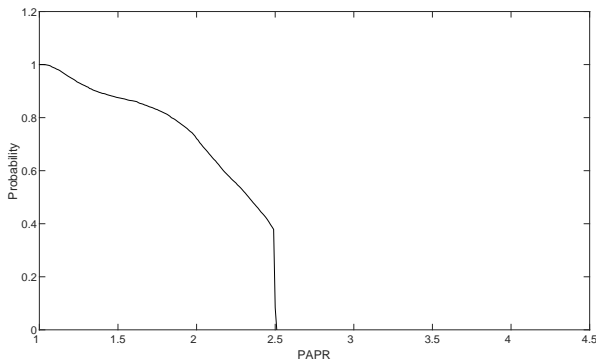
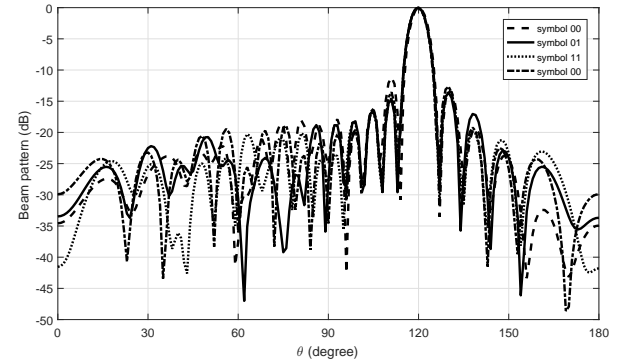


FIGURE 5: CCDF of PAPR based on broadside design using eq. (20) when $\rho = 2.5$.

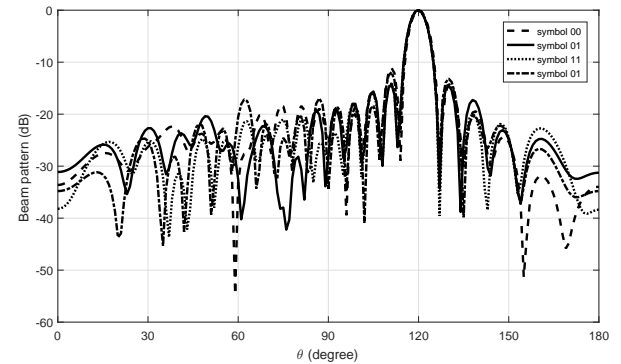
design examples are provided. In the broadside design example, the mainlobe direction is assumed to be $\theta_{ML} = 90^\circ$ and the sidelobe regions are $\theta_{SL} \in [0^\circ, 85^\circ] \cup [95^\circ, 180^\circ]$, sampled every 1° . In the off-broadside design example, $\theta_{ML} = 120^\circ$ and $\theta_{SL} \in [0^\circ, 115^\circ] \cup [125^\circ, 180^\circ]$, sampled every 1° . The carrier frequency f_0 is set to 2.4GHz, with a bandwidth of 1.25MHz split into $Q = 4$ frequencies (4-point IDFT). For each frequency, the desired response is a value of one (magnitude) with 90° phase shift at the mainlobe, i.e. QPSK where the constellation points are at $45^\circ, 135^\circ, -135^\circ, -45^\circ$ for symbols ‘00’, ‘01’, ‘11’, ‘10’, and a value of 0.1 (magnitude) with random phase over the sidelobe regions. The threshold of the PAPR is set to $\rho = 2.5$. The value of denominator $f'(\{\psi_q\}_{q=-Q/2}^{Q/2-1})$ is set to be 4 by trial and error, and the value smaller than this cannot guarantee the convergence of (22).

Moreover, complementary cumulative distribution function (CCDF) [30] is used to show the probability (PR) of PAPRs exceeding a given value

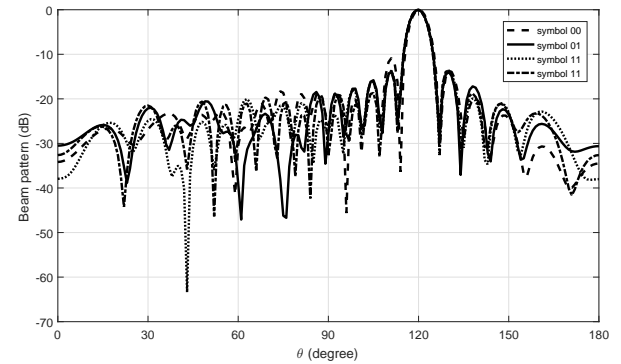
$$\begin{aligned} \text{PR}(\text{PAPR} > \text{PAPR}_{\text{value}}) \\ = 1 - \text{PR}(\text{PAPR} \leq \text{PAPR}_{\text{value}}) \end{aligned} \quad (25)$$



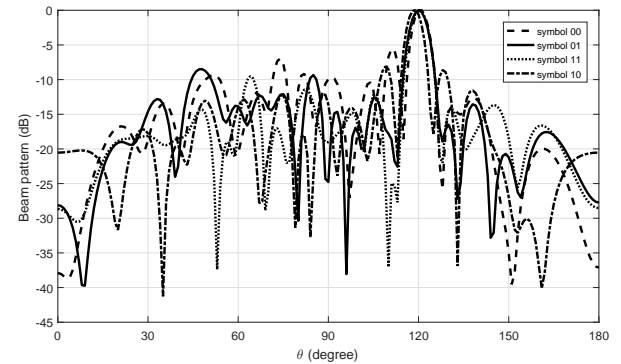
(a)



(b)



(c)



(d)

FIGURE 6: Resultant beam responses based on the off-broadside design using eq. (20) for symbols (a) ‘00,01,11,00’, (b)‘00,01,11,01’, (c)‘00,01,11,11’, (d)‘00,01,11,10’ when $\rho = 2.5$.

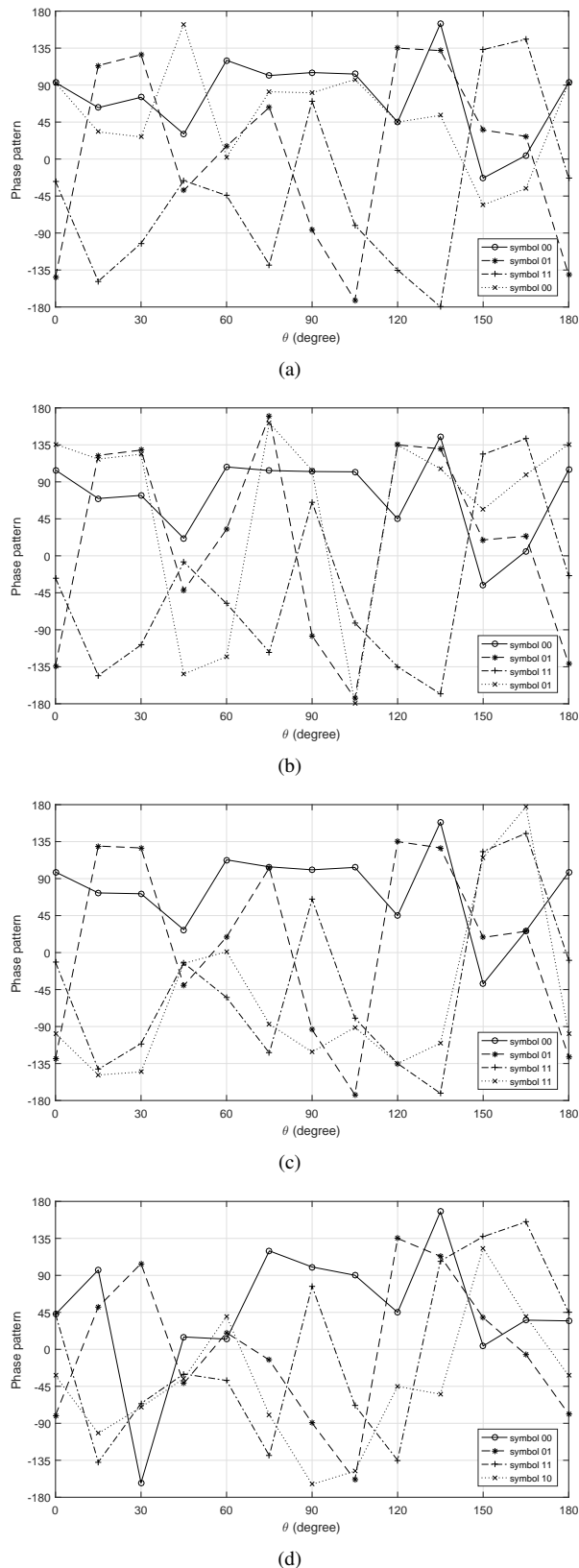


FIGURE 7: Resultant phase patterns based on the off-broadside design using eq. (20) for symbols (a) ‘00,01,11,00’, (b) ‘00,01,11,01’, (c) ‘00,01,11,11’, (d) ‘00,01,11,10’ when $\rho = 2.5$.

A. BROADSIDE DESIGN EXAMPLE WITHOUT PAPR CONSTRAINT

The resultant beam patterns using (5) without PAPR constraint at frequencies $f_0 - 2\Delta f$, $f_0 - \Delta f$, f_0 and $f_0 + \Delta f$ are shown in Fig. 2 for symbols ‘00,01,11,00’, ‘00,01,11,01’, ‘00,01,11,11’, ‘00,01,11,10’, and the corresponding phase patterns are displayed in Fig. 3. It can be seen that all main beams are exactly pointed to $\theta = 90^\circ$ (desired direction) with a reasonable sidelobe level, and the phase in the main beam direction follows the given QPSK constellation diagram and random over the sidelobe ranges. The beam and phase patterns for other symbols are not shown as they have the same features as the aforementioned figures. Moreover, as shown in Fig. 4, the values of PAPR for all sets of inputs are in the range of [1, 4].

B. BROADSIDE DESIGN EXAMPLE SUBJECT TO $PAPR \leq \rho$

The resultant beam and phase patterns for all symbols under $PAPR \leq 2.5$ by (20) is similar to the design without PAPR consideration, as shown in Figs. 2 and 3, where all main beams are pointed to the desired direction $\theta = 90^\circ$ with a given shift, and random phase shift over sidelobe range with a low magnitude, demonstrating the satisfaction of the DM requirements. The CCDF of the PAPRs for all sets of inputs in this design is shown in Fig. 5. Here it can be seen that the probability of PAPR is down to zero when the PAPR is over the pre-defined threshold $\rho = 2.5$, indicating that the PAPR constraint has been met in the design.

C. OFF-BROADSIDE DESIGN EXAMPLE SUBJECT TO $PAPR \leq \rho$

The resultant beam patterns for these four symbols are shown in Fig. 6, where all the main beams are pointed to the desired direction $\theta = 120^\circ$ with low sidelobe level in other directions. The corresponding phase patterns are displayed in Fig. 7, where it can be seen that in the desired direction 120° the phases for these symbols are the same as the required QPSK modulation pattern, while in other directions the phase values are random. The beam and phase patterns for other symbols have the DM characteristics as well. The corresponding CCDF of PAPRs for all sets of inputs is similar to the broadside design with PAPR consideration, as shown in Fig. 5, where the range of PAPR for off-broadside design is [1,2.5]; in other words, PAPR constraints $PAPR \leq 2.5$ has been satisfied.

V. CONCLUSIONS

In this paper, to solve the potential high peak to average power ratio problem in the antenna array design for IDFT based multi-carrier directional modulation, a method called wideband beam and phase pattern formation by Newton’s method (WBPFN) has been proposed for the first time to meet both the DM requirement and the PAPR constraint. As shown in the provided broadside and off-broadside design examples, the main beams of the design results have pointed

to the desired direction and the phase responses followed the given constellation diagram in the mainlobe and random in the sidelobe, providing an effective directional modulation performance. Moreover, the CCDF results has demonstrated clearly that the PAPR requirement has been met effectively by the proposed method.

REFERENCES

- [1] A. Babakhani, D. B. Rutledge, and A. Hajimiri. "Transmitter architectures based on near-field direct antenna modulation". *IEEE Journal of Solid-State Circuits*, 43(12):2674–2692, December 2008.
- [2] A. Babakhani, D. B. Rutledge, and A. Hajimiri. "Near-field direct antenna modulation". *IEEE Microwave Magazine*, 10(1):36–46, February 2009.
- [3] M. P. Daly and J. T. Bernhard. "Beamsteering in pattern reconfigurable arrays using directional modulation". *IEEE Transactions on Antennas and Propagation*, 58(7):2259–2265, March 2010.
- [4] T. Hong, M. Z. Song, and Y. Liu. "Dual-beam directional modulation technique for physical-layer secure communication". *IEEE Antennas and Wireless Propagation Letters*, 10:1417–1420, December 2011.
- [5] M. P. Daly and J. T. Bernhard. "Directional modulation technique for phased arrays". *IEEE Transactions on Antennas and Propagation*, 57(9):2633–2640, September 2009.
- [6] M. P. Daly and J. T. Bernhard. "Directional modulation and coding in arrays". In *Proc. IEEE International Symposium on Antennas and Propagation (APSURSI)*, pages 1984–1987, Spokane, WA, USA, July 2011.
- [7] H. Z. Shi and A. Tennant. "Enhancing the security of communication via directly modulated antenna arrays". *IET Microwaves, Antennas & Propagation*, 7(8):606–611, June 2013.
- [8] M. B. Hawes and W. Liu. "Compressive sensing based approach to the design of linear robust sparse antenna arrays with physical size constraint". *IET Microwaves, Antennas & Propagation*, 8(10):736–746, July 2014.
- [9] Y. Ding and V. Fusco. "A vector approach for the analysis and synthesis of directional modulation transmitters". *IEEE Transactions on Antennas and Propagation*, 62(1):361–370, January 2014.
- [10] Y. Ding and V. Fusco. "Directional modulation far-field pattern separation synthesis approach". *IET Microwaves, Antennas & Propagation*, 9(1):41–48, 2015.
- [11] B. Zhang, W. Liu, and X. M. Gou. "Compressive sensing based sparse antenna array design for directional modulation". *IET Microwaves, Antennas & Propagation*, 11(5):634–641, April 2017.
- [12] B. Zhang, W. Liu, and X. Lan. "Directional modulation design based on crossed-dipole arrays for two signals with orthogonal polarisations". In *Proc. European Conference on Antennas and Propagation (EuCAP)*, London, UK, April 2018.
- [13] B. Zhang and W. Liu. "Antenna array based positional modulation with a two-ray multi-path model". In *2018 IEEE 10th Sensor Array and Multichannel Signal Processing Workshop (SAM)*, pages 203–207, July 2018.
- [14] Y. Ding and V. Fusco. "Directional modulation transmitter radiation pattern considerations". *IET Microwaves, Antennas & Propagation*, 7(15):1201–1206, December 2013.
- [15] Q. J. Zhu, S. W. Yang, R. L. Yao, and Z. P. Nie. "Directional modulation based on 4-D antenna arrays". *IEEE Transactions on Antennas and Propagation*, 62(2):621–628, February 2014.
- [16] T. Xie, J. Zhu, and Y. Li. "Artificial-noise-aided zero-forcing synthesis approach for secure multi-beam directional modulation". *IEEE Communications Letters*, 22(2):276–279, February 2018.
- [17] B. Zhang and W. Liu. "Multi-carrier based phased antenna array design for directional modulation". *IET Microwaves, Antennas & Propagation*, 12(5):765–772(7), April 2018.
- [18] L. Litwin and M. Pugal. "The principles of OFDM". *RF signal processing*, 2:30–48, January 2001.
- [19] Y. Kou, W. S. Lu, and A. Antoniou. "New peak-to-average power-ratio reduction algorithms for multicarrier communications". *IEEE Transactions on Circuits and Systems I: Regular Papers*, 51(9):1790–1800, September 2004.
- [20] V. Chakravarthy, A. S. Nunez, J. P. Stephens, A. K. Shaw, and M. A. Temple. "TDCS, OFDM, and MC-CDMA: a brief tutorial". *IEEE Communications Magazine*, 43(9):S11–S16, September 2005.
- [21] Y. S. Cho, J. Kim, W. Y. Yang, and C. G. Kang. "Introduction to OFDM", pages 111–151. John Wiley & Sons, Ltd, August 2010.
- [22] L. Hanzo, Y. (Jos) Akhtman, L. Wang, and M. Jiang. "Introduction to OFDM and MIMO-OFDM", pages 1–36. Wiley-IEEE Press, 2011.
- [23] A. Gangwar and M. Bhardwaj. "An overview: Peak to average power ratio in OFDM system & its effect". *International Journal of Communication and Computer Technologies*, 1(2):22–25, September 2012.
- [24] S. Sharma and P. K. Gaur. "Survey on PAPR reduction techniques in OFDM system". *International Journal of Advanced Research in Computer and Communication Engineering*, 4(6):271–274, June 2015.
- [25] M. Bala, M. Kumar, and K. Rohilla. "PAPR reduction in OFDM signal using signal scrambling techniques". *International Journal of Engineering and Innovative Technology (IJET)*, 3(11):140–143, May 2014.
- [26] M. Mohamad, R. Nilsson, and J. van de Beek. "A novel transmitter architecture for spectrally-precoded OFDM". *IEEE Transactions on Circuits and Systems I: Regular Papers*, pages 1–14, February 2018.
- [27] X. D. Li and L. J. Cimini. "Effects of clipping and filtering on the performance of OFDM". *IEEE Communications Letters*, 2(5):131–133, May 1998.
- [28] X. Zhu, W. Pan, H. Li, and Y. Tang. "Simplified approach to optimized iterative clipping and filtering for PAPR reduction of OFDM signals". *IEEE Transactions on Communications*, 61(5):1891–1901, May 2013.
- [29] R. W. Bauml, R. F. H. Fischer, and J. B. Huber. "Reducing the peak-to-average power ratio of multicarrier modulation by selected mapping". *Electronics Letters*, 32(22):2056–2057, October 1996.
- [30] W. X. Lin, J. C. Lin, and Y. T. Sun. "Modified selective mapping technique for PAPR reduction in OFDM systems". In *Proc. International Conference on ITS Telecommunications*, pages 764–768, Taipei, China, November 2012.
- [31] S. H. Muller and J. B. Huber. "OFDM with reduced peak-to-average power ratio by optimum combination of partial transmit sequences". *Electronics Letters*, 33(5):368–369, February 1997.
- [32] J. C. Chen. "Partial transmit sequences for PAPR reduction of OFDM signals with stochastic optimization techniques". *IEEE Transactions on Consumer Electronics*, 56(3):1229–1234, August 2010.
- [33] S. Hu, G. Wu, Q. S. Wen, Y. Xiao, and S. Q. Li. "Nonlinearity reduction by tone reservation with null subcarriers for WiMAX system". *Wireless Personal Communications*, 54(2):289–305, July 2010.
- [34] N. Jacklin and Z. Ding. "A linear programming based tone injection algorithm for PAPR reduction of OFDM and linearly precoded systems". *IEEE Transactions on Circuits and Systems I: Regular Papers*, 60(7):1937–1945, July 2013.
- [35] H. He, P. Stoica, and J. Li. "Wideband MIMO systems: Signal design for transmit beam pattern synthesis". *IEEE Transactions on Signal Processing*, 59(2):618–628, February 2011.
- [36] H. He, P. Stoica, and J. Li. "On aperiodic-correlation bounds". *IEEE Signal Processing Letters*, 17(3):253–256, March 2010.
- [37] J. A. Tropp, I. S. Dhillon, R. W. Heath, and T. Strohmer. "Designing structured tight frames via an alternating projection method". *IEEE Transactions on Information Theory*, 51(1):188–209, January 2005.



sparse array design.

BO ZHANG received his BSc from Tianjin Normal University, China, in 2011. MSc and PhD from the Department of Electrical and Electronic Engineering, University of Sheffield in 2013 and 2018, respectively.

He is working with the College of Electronic and Communication Engineering, Tianjin Normal University. His research interests cover array signal processing (beamforming and direction of arrival estimation, etc.), directional modulation and



WEI LIU (S'01-M'04-SM'10) received his BSc and LLB. degrees from Peking University, China, in 1996 and 1997, respectively, MPhil from the University of Hong Kong in 2001, and PhD from the School of Electronics and Computer Science, University of Southampton, UK, in 2003. He then worked as a postdoc first at Southampton and later at the Department of Electrical and Electronic Engineering, Imperial College London.

Since September 2005, he has been with the Department of Electronic and Electrical Engineering, University of Sheffield, UK, first as a Lecturer and then a Senior Lecturer. He has published more than 250 journal and conference papers, three book chapters, and a research monograph about wideband beamforming "Wideband Beamforming: Concepts and Techniques" (John Wiley, March 2010). Another book titled "Low-Cost Smart Antennas" (by Wiley-IEEE) will appear in March 2019. His research interests cover a wide range of topics in signal processing, with a focus on sensor array signal processing (beamforming and source separation/extraction, direction of arrival estimation, target tracking and localisation, etc.), and its various applications, such as robotics and autonomous vehicles, human computer interface, big data analytics, radar, sonar, satellite navigation, and wireless communications.

He is a member of the Digital Signal Processing Technical Committee of the IEEE Circuits and Systems Society and the Sensor Array and Multichannel Signal Processing Technical Committee of the IEEE Signal Processing Society (Vice-Chair from Jan 2019). He is currently an Associate Editor for IEEE Trans. on Signal Processing and IEEE Access, and an editorial board member of the Journal Frontiers of Information Technology and Electronic Engineering.



QIANG LI received the B.Eng. degree in electronic engineering from Henan University of Science and Technology, China, in 2010, and the Ph.D. degree in control science and engineering from Harbin Engineering University, China, in 2015. From 2015-2016, he was employed at Shenzhen University, China, where he worked on frequency diverse array and space-time adaptive processing. He joined communication group of the University of Sheffield, UK, in 2016, as a visiting scholar,

where he researched the phase retrieval algorithms for antenna array. From 2018-now, he was employed at Shenzhen University as associate researcher, where he researched the optimization theory.

...